J. Membrane Biol. 11, 293 – 308 (1973)


# The Nature of Passive Flows through Tightly Folded Membranes

## The Influence of Microstructure

I. W. Richardson, Vojtech Ličko, and Ettore Bartoli

Cardiovascular Research Institute and Departments of Medicine, Physiology, and Biochemistry and Biophysics, University of California, San Francisco, California 94122

Received 2 August 1972

*Summary.* Membrane processes such as microvilli and folded structures greatly increase the area for passive transport. A mathematical analysis of flows through folded membrane structures demonstrates that the increase in flows is not proportional to the increase in area. Furthermore, the flows of salt and water do not increase in the same ratio: that of water can be several times the increase in area and that of salt a fraction of the increase in area. A preferential passive flow of water is created by the structure. It is only in the neighborhood of the isotonic state that the effect is significant, but in that region, the effect can be dramatic.

A parameter study shows that the effect is most sensitive to the relative dimensions of the folded membrane structure and to the salt permeability. The effect of stirring within the folds is also studied. In the general case, the system of two-dimensional diffusion equations is integrated numerically; an analytical solution is presented for the special case of negligible convection coupling. The calculations show that salt-concentration profiles within the folds establish a distribution of thermodynamic driving forces across the membrane barrier which differs significantly from that found across a plane membrane separating the same bathing solutions. The overall behavior of the flows through folded membrane structures is thus nonlinear.

Structural processes of membranes such as microvilli obviously affect the passive flows of solutes and water by providing a greatly increased surface area. However, it must not be concluded that the flows necessarily increase in direct proportion to the area increase or even that the solute flow and the water flow increase in the same ratio. Important qualitative effects accompany the quantitative effects produced by the microstructure; there is an alteration in the very nature of the relationships between the flows and the thermodynamic driving forces as measured in the two bathing solutions separated by the membrane structure. In the steady state, con-

centration gradients are established in the membrane folds, giving continuous and nonlinear distributions for the driving forces across the membrane. The influence of the microstructure is dramatic; in a typical case where the infolding increased the membrane area by a factor of 34, the increase in solute flow was only 31 whereas the increase in water flow was 110.

It is the microgeometry of the structure as well as the permeabilities of the membrane composing the structure that dictate the nature of the flows through a folded membrane. In fact, we must make a clear distinction between the membrane and the structure. In the steady state, the flow properties of the *membrane* are completely characterized by the phenomenological coefficients of Kedem and Katchalsky (1963) if the thickness of the membrane is small enough, as compared to the radii of curvature of the membrane surface, to allow one-dimensional transmembrane flow equations. At any point of the membrane structure the local flows of salt and volume are given by the well-known *practical* equations given here as Eqs. (8) and (9). These equations, however, do not describe the overall behavior of flows through folded membranes. And, as will be seen, a value of the linear flow coefficients $\omega$, $L_P$, or $\sigma$ obtained in the usual manner as a ratio of flow-to-force (e.g., $\omega = J_s/\Delta\Pi_s$ at $J_V = 0$) is essentially meaningless for these nonlinear systems.

To discover the nature of flows through a folded membrane, we must solve a system of differential flow equations allowing for the two-dimensional flows into the small regions delimited by the folds of the membrane, their passage through the membrane, and their exit out the conjugated small regions on the opposite side of the membrane. A parameter study shows how the overall flows through a folded membrane depend upon the membrane's phenomenological coefficients, the concentrations in the bathing solutions, and the dimensions of the structure. The flows are compared to those through a similar plane membrane, normalized to account for the increase in area. For the parameter studies, the system equations are solved numerically; an analytical solution is presented for the restricted case of negligible convection coupling.

## Physical Model

The simplest geometry which retains the essential features common to three-dimensional figures such as brush borders and two-dimensional folded structures is the folded membrane shown in Fig. 1*a*. In fact, to avoid mathematical complexities, we shall simplify this to the degree shown in the cross-section presented in Fig. 1*b*. The folded membrane separates two

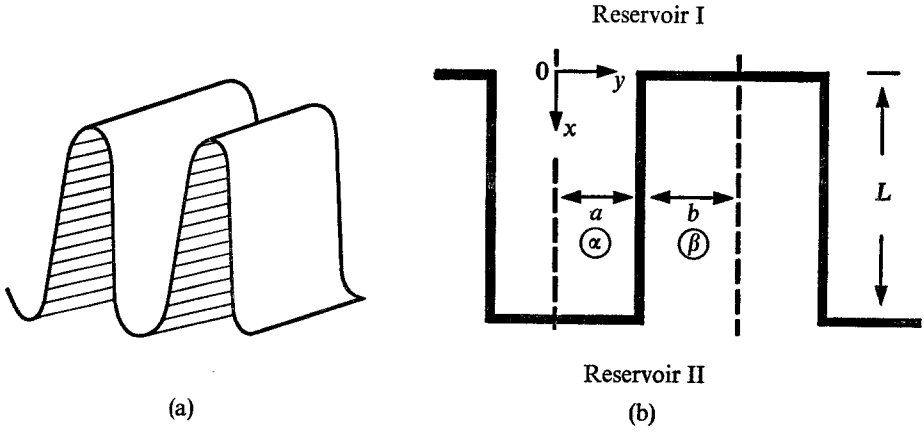


Fig. 1. Perspective view (*a*) and schematic drawing (*b*) of a folded membrane. Only the section depicted between the two dashed lines need be considered in the analysis because of the symmetry and periodicity of the structure

large, well-stirred reservoirs, I and II; this would represent, for example, a biological system in which a low intracellular sodium concentration is maintained constant by a pump in another region of the plasma membrane. The breadth of the folded strip of membrane is unity, and there is no diffusion along the z-axis, all concentrations being constant in that direction; in other words, we consider one centimeter of a structure extending infinitely along the z-axis. Positive flows proceed from reservoir I into the small region of width $2a$, through the membrane into the small region of width $2b$, and finally out into reservoir II.

Because of geometric symmetry, we need study only half of a cell delimited by the folds. The region of interest is marked off by dashed lines in Fig. 1*b*. This figure also establishes the origin and orientation of the coordinate system.

## Mathematical Model

Because of the relative dimensions of the structure, we can write a set of system equations which, although not simple, are far less complicated than those which would arise from a straightforward application of the Equation of Continuity to the two-dimensional vectors of salt and volume flow in regions $\alpha$ and $\beta$ and the consideration of suitable continuity conditions at the membrane-solution interfaces. The mathematical economy effected by our assumptions will become evident as we proceed.

To write the basic conservation equation we consider the salt flows into and out of the differential volume shown in Fig. 2. Implicit in the figure is

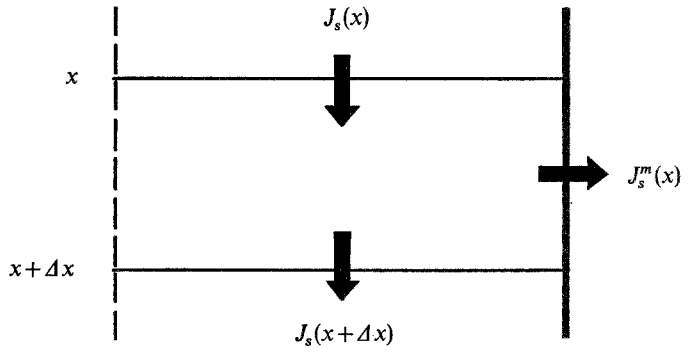


Fig. 2. Schematic representation of the flows in a differential section of region $\alpha$

the observation that the half-width, $\Delta y = a$, of region $\alpha$ is small compared to the length $L$ which is divided into intervals of $\Delta x$. By symmetry the $y$-component of the salt flow is zero at $y = 0$. At steady state there is no local accumulation of salt, and so the flux into the differential volume must be balanced by the flux out: i.e.,

$$J_s^\alpha(x)a = J_s^\alpha(x+\Delta x)a + J_s^m(x)\Delta x \tag{1}$$

where $J_s^\alpha(x) = x$-component of the salt flow in region $\alpha$ and $J_s^m(x) =$ salt flow through the membrane. Dividing Eq. (1) by $a\Delta x$ and taking the limit as $\Delta x \to 0$ gives the conservation equation

$$\frac{dJ_s^\alpha}{dx} + \frac{J_s^m}{a} = 0. \tag{2}$$

There is no electrical current flow; the salt moves down region $\alpha$ by diffusion and convection, obeying the following flow equation:

$$J_s^\alpha = -D_s \frac{dC_s^\alpha}{dx} + C_s^\alpha J_V^\alpha \tag{3}$$

where $D_s =$ salt diffusion coefficient, $C_s^\alpha = C_s^\alpha(x) =$ salt concentration in region $\alpha$, and $J_V^\alpha = J_V^\alpha(x) =$ flow of volume in region $\alpha$. Rather than specify an equation describing the flow of volume in region $\alpha$, we use a conservation statement:

$$J_V^\alpha = \frac{1}{a}\int_x^L J_V^m(\xi)\,d\xi + J_V^m \text{ (end plate of region } \alpha) \tag{4}$$

where $J_V^m = J_V^m(x)$ is the volume flow through the membrane. The analogous equation for region $\beta$ is

$$J_V^\beta = \frac{1}{b}\int_0^x J_V^m(\xi)\,d\xi + J_V^m \text{ (end plate of region } \beta). \tag{5}$$

Thus, Eq. (2) can be written as

$$-D_s\frac{d^2C_s^\alpha}{dx^2}+\frac{dC_s^\alpha}{dx}J_V^\alpha-\frac{C_s^\alpha J_V^m}{a}+\frac{J_s^m}{a}=0, \tag{6}$$

and similarly

$$-D_s\frac{d^2C_s^\beta}{dx^2}+\frac{dC_s^\beta}{dx}J_V^\beta+\frac{C_s^\beta J_V^m}{b}-\frac{J_s^m}{b}=0. \tag{7}$$

The flows through the membrane at any given value of $x$ are given by the Kedem-Katchalsky equations as

$$J_V^m=L_P(\Delta P-\Delta\Pi_i-\sigma\Delta\Pi_s) \tag{8}$$

and

$$J_s^m=\omega\Delta\Pi_s+\bar{C}_s(1-\sigma)J_V^m \tag{9}$$

where $L_P$ = hydraulic permeability, $\Delta P=P^\alpha-P^\beta$ = hydrostatic pressure difference, $\Delta\Pi_i=RT(C_i^\alpha-C_i^\beta)$ = osmotic driving force of impermeant species, $\sigma$ = reflection coefficient, $\Delta\Pi_s=2RT(C_s^\alpha-C_s^\beta)$ = osmotic driving force of salt, $\omega$ = salt permeability, and $\bar{C}_s=\frac{C_s^\alpha+C_s^\beta}{2}$. The system Eqs. (6) and (7) are augmented by two flow equations for the impermeant species in regions $\alpha$ and $\beta$:

$$-D_i\frac{dC_i^\alpha}{dx}+C_i^\alpha J_V^\alpha=0 \tag{10}$$

and

$$-D_i\frac{dC_i^\beta}{dx}+C_i^\beta J_V^\beta=0 \tag{11}$$

where $D_i$ = diffusion coefficient for impermeant species and $C_i=C_i(x)$ = concentration of impermeant species.

An integration of the system Eqs. (6) through (11) gives rise to six constants which are dependent upon the boundary conditions. On the boundaries of the physical model, four concentrations are immediately determined by the values in reservoirs I and II: i.e.,

$$\begin{aligned} &C_s^\alpha(0)=C_s^{\mathrm{I}}, \qquad C_i^\alpha(0)=C_i^{\mathrm{I}} \\ \text{and} \qquad &C_s^\beta(L)=C_s^{\mathrm{II}}, \qquad C_i^\beta(L)=C_i^{\mathrm{II}}. \end{aligned} \tag{12}$$

Boundary values for the concentration gradients are obtained from a consideration of the flows at the two end plates of the structure: that is, at $x=L$ in region $\alpha$ and at $x=0$ in region $\beta$. The flow of the permeant salt must be continuous across the end plates of the membrane, and thus the boundary values of the salt concentration gradients are obtained from the

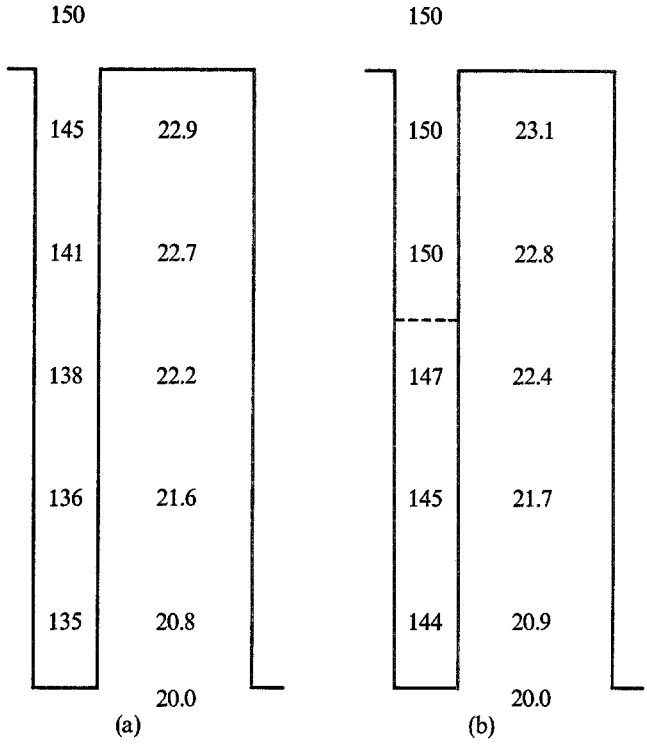


Fig. 3. Concentration profiles in a folded membrane (*a*). In (*b*) the solution in region $\alpha$ is stirred for 40% of the length of the folds. The numbers are the concentrations of the permeant salt in millimoles, starting with 150 mM in reservoir I and ending with 20 mM in reservoir II. The folds are not drawn to scale, though their dimensions are indicative of the ratios between the length and widths of the folds

condition

$$J_s^{\alpha}(L) = J_s^m \text{ (end plate of region } \alpha) \\ = \omega \Delta \Pi_s + \bar{C}_s(1-\sigma) J_V^m \text{ evaluated at the end plate of region } \alpha \tag{13}$$

along with the analogous equation for region $\beta$. Eq. (3) gives $J_s^{\alpha}(L)$, and on the right-hand side of Eq. (13) the quantities are calculated using the concentration values $C_s^{\alpha}(L)$ and $C_s^{\mathrm{II}}$: e.g., $\Delta \Pi_s = 2RT[C_s^{\alpha}(L) - C_s^{\mathrm{II}}]$.

Appendix I outlines the procedure used to solve the system equations on a digital computer. The system equations are nonlinear because of the convection-coupling term in the salt flow equations. In most biological situations the relative magnitudes of $\omega$ and $L_P$ result in negligible convection coupling. In that case, the system Eqs. (6) and (7) reduce to a linear fourth-order system of ordinary differential equations, and a closed-form solution is possible. Although the solution is cumbersome once the boundary

values are incorporated into it, the characteristic values are themselves of interest, indicating in brief how the system parameters determine the gross behavior of the system. The closed-form solution is presented in Appendix II.

With a single adjustment of one boundary condition, we can study the effects of stirring. In folded membranes there are unstirred chambers, in contrast to the unstirred layers of plane membranes. In the example depicted in Fig. 3*a*, the stirring in reservoir I is sufficient to maintain a constant concentration in the reservoir up to the mouth of region $\alpha$. For the sake of the example, let us postulate a salt concentration of 150 mM in reservoir I; therefore the concentration at $x=0$ is $C_s^{\alpha}(0)=C_s^{\mathrm{I}}=150$ mM. If, however, the stirring becomes more vigorous, the fluid in the mouth of region $\alpha$ is also stirred, and the concentration is 150 mM for some distance into region $\alpha$. Mathematically we have $C_s^{\alpha}(x)=C_s^{\mathrm{I}}$ for $0\leqq x\leqq x^*$ where $x^*$ is the extent of the stirred region. Fig. 3*b* shows the concentration profile obtained when $x^*=0.4\,L$ and all other system parameters correspond to those of the "standard" case given in Results.

## Results

The large number of parameters required to characterize a folded membrane precludes a study of the system for all combinations of parameters. Therefore we have chosen a set of arbitrary, but biologically plausible, parameters which we refer to as the "standard" case; from this basis we proceed to investigate the behavior of the system by varying one parameter at a time. The "standard" folded membrane is characterized by the following values:

| | | |
|---|---|---|
| $L=2\times10^{-4}$ cm | $L_P=4\times10^{-13}$ cm³/dyne-sec | $D_i=0.5\times10^{-5}$ cm²/sec |
| $a=1\times10^{-6}$ cm | $P_s=2RT\omega=8\times10^{-5}$ cm/sec | $D_s=1.5\times10^{-5}$ cm²/sec |
| $b=5\times10^{-6}$ cm | $\sigma=0.7$ | $\Delta P=0.$ |
| $C_s^{\mathrm{I}}=150$ mM | $C_i^{\mathrm{I}}=0$ | |
| $C_s^{\mathrm{II}}=20$ mM | $C_i^{\mathrm{II}}=190$ mM | |

Note that the salt permeability of the membrane is listed in the units most familiar to physiologists, cm/sec. The value $C_s^{\mathrm{II}}=190$ mM was chosen with the desire to keep the system nearly isotonic; for $C_i^{\mathrm{II}}=182$ mM the system would, in fact, be isotonic for a plane membrane having the preceding transport coefficients. However, we wish to compare by ratios the flows

through a folded membrane with those through the corresponding plane membrane. Hence we must avoid the zero divisor arising from $J_V = 0$ for an isotonic plane membrane. The value for $C_i^{II}$ was therefore rounded off to 190 mM, giving for the plane membrane an effective osmotic driving force of 8 milliosmoles.

For evaluating the performance of a folded membrane, a relative measure is far more informative than plots of absolute flows versus the particular parameter being varied. The results of the calculations are presented here as (1) $R_V$, the ratio of volume flow for the folded membrane to that for the plane membrane of the same total surface area; (2) $R_s$, the corresponding ratio of salt flows; and (3) $R_V/R_s$, the ratio of the two preceding ratios, which we shall call the concentrating ratio. As will be seen, the ratio of volume flows is never smaller than one, while the ratio of salt flows is never

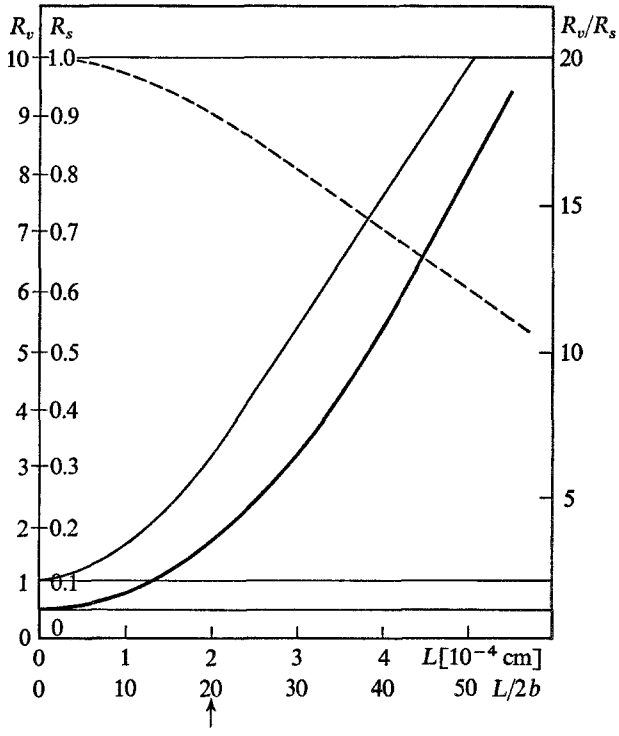


Fig. 4. The ratios of flows for a folded membrane compared with those for a plane membrane of equal area as functions of the length $L$ and of the relative measure of length-to-width, $L/2b$. The narrow line is the volume flow ratio, $R_V = J_V$(folded)/$J_V$(plane); the dashed line is the salt flow ratio, $R_s = J_s$(folded)/$J_s$(plane); and the wide line is the concentrating ratio, $R_V/R_s$. The three curves are plotted to different scales. The horizontal lines are unit ratios. The arrow indicates the length of the "standard" folded membrane

greater than one; it follows that the concentrating ratio never becomes less than one. All ratios are unity if the only effect arising from the microstructure is an increase in area.

### *Influence of Geometry*

The first parameter study is a variation of the length $L$ of the folds; the half-widths, $a$ and $b$, of regions $\alpha$ and $\beta$ delimited by the folds are kept constant at the "standard" values. At $L=0$, the structure reduces to a plane membrane, and all flow ratios are unity. As seen in Fig. 4, the flow ratios remain essentially unity until the length-width ratio ($L/b$) becomes about 10; at that point the influence of the geometry of the microstructure becomes evident, with a region of rapid variation in the flow ratios. Beyond this region the ratios are more or less a linear function of the length $L$.

For a fixed $L$ corresponding to the "standard" case, the effects of varying the ratio of the widths of regions $\alpha$ and $\beta$ (i.e., $a/b$) were studied. The flow ratios are shown in Fig. 5.

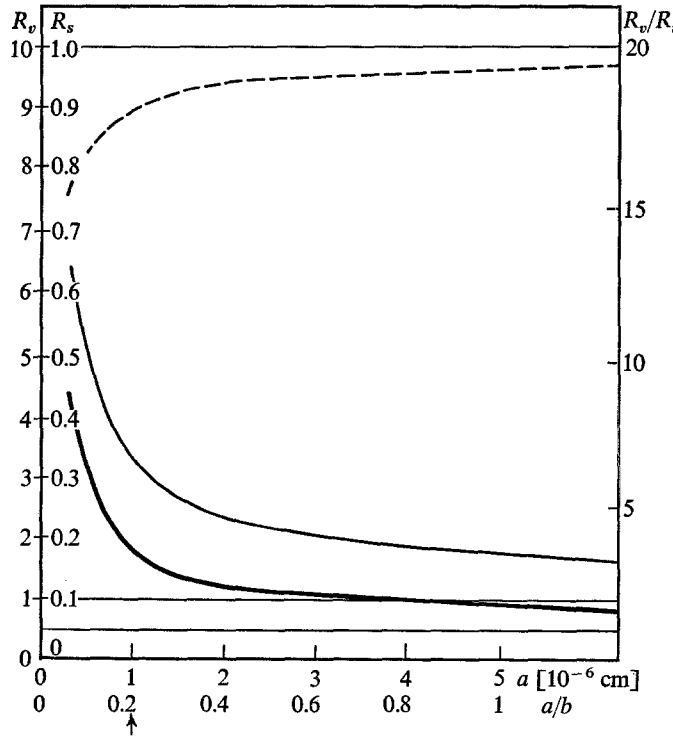


Fig. 5. The flow ratios as functions of the half-width $a$ of region $\alpha$ and of the relative measure $a/b$. The narrow line is $R_V$; the dashed line is $R_s$; and the wide line is $R_V/R_s$

*Influence of Membrane Transport Coefficients*

The system is very sensitive to the value of the salt permeability, $\omega$. In Fig. 6 the flow ratios are plotted for variations in salt permeability, given in units of cm/sec as $P_s = 2RT\omega$. Except for an increase in area, there is no effect of microstructure for permeability values of the order associated with tight membranes such as those of the nerve: $10^{-7} \leqq P_s \leqq 10^{-5}$ cm/sec. However, for highly permeable membranes such as those of the proximal tubule or the intestine ($P_s > 10^{-5}$ cm/sec), the behavior of a folded membrane is quite different from that of a plane membrane, water transport being greatly increased and salt transport decreased.

Since the reflection coefficient $\sigma$ is a determining factor in the calculation of the near isotonic conditions we imposed upon the "standard" case, it was impossible to vary $\sigma$ independently. Therefore, the salt concentrations were maintained at $C_s^{\mathrm{I}} = 150$ mM and $C_s^{\mathrm{II}} = 20$ mM, while for each value of $\sigma$ the concentration $C_i^{\mathrm{II}}$ was adjusted to give an effective osmotic driving force of 8 milliosmoles for the plane membrane. With this constraint the variation

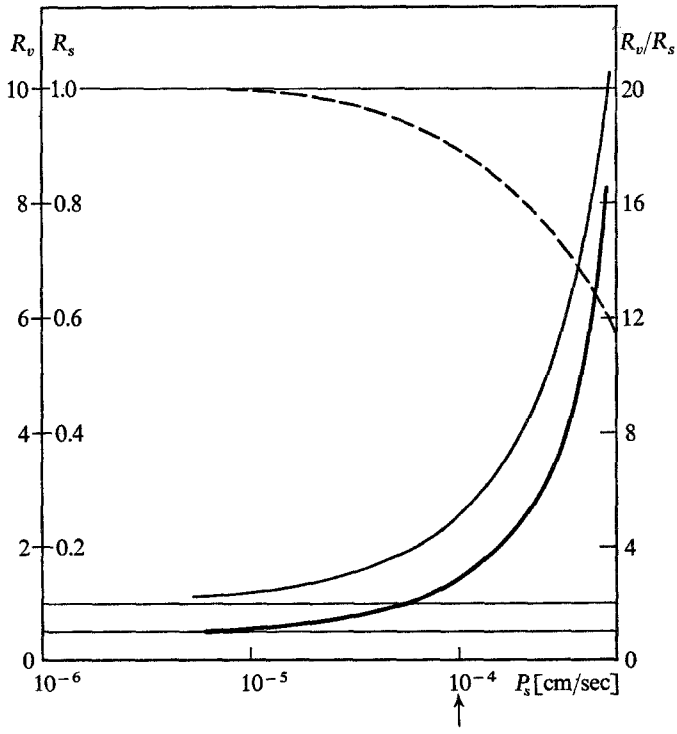


Fig. 6. The flow ratios as functions of the permeability coefficient, $P_s$. The narrow line is $R_V$; the dashed line is $R_s$; and the wide line is $R_V/R_s$

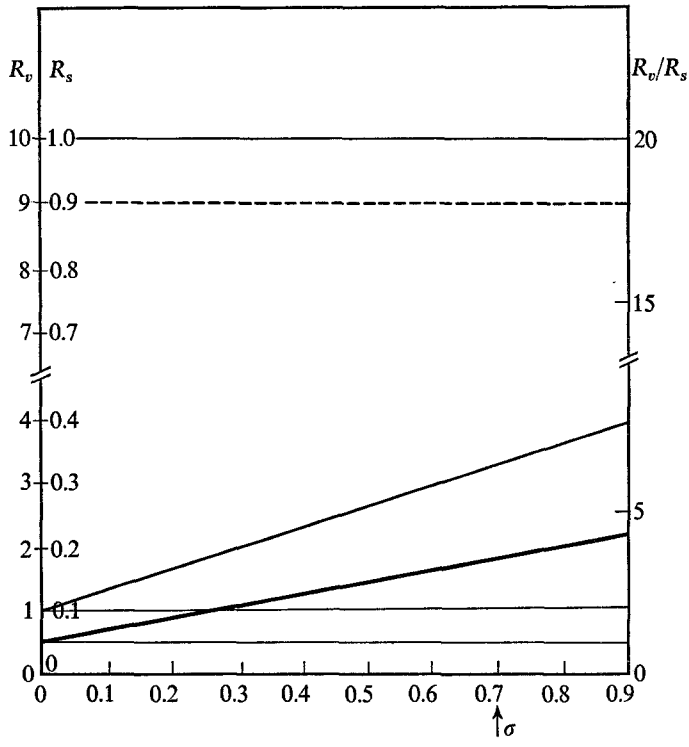


Fig. 7. The flow ratios as functions of the reflection coefficient $\sigma$. The narrow line is $R_V$; the dashed line is $R_s$; and the wide line is $R_V/R_s$

of $\sigma$ produces a linear increase in $R_V$, as shown in Fig. 7. The salt flow ratio remains constant for $0 \leqq \sigma \leqq 1$.

Variations in the hydraulic permeability $L_P$ have no effect upon the overall behavior of folded membranes. The flow ratios are unchanged over a variation in $L_P$ of many orders of magnitude. Because of the relative magnitudes of $L_P$ and the "standard" value of $\omega$, there is almost no convection coupling, and hence volume flow plays no part in the establishment of concentration profiles in regions $\alpha$ and $\beta$.

### *Role of the Impermeant Species*

The unusual behavior of folded membranes occurs because the membrane separates two small regions wherein concentration gradients are established, thus giving local driving forces different from those measured in the bathing solutions. For all cases presented in the parameter study, convection coupling was negligible, and hence the concentration of the

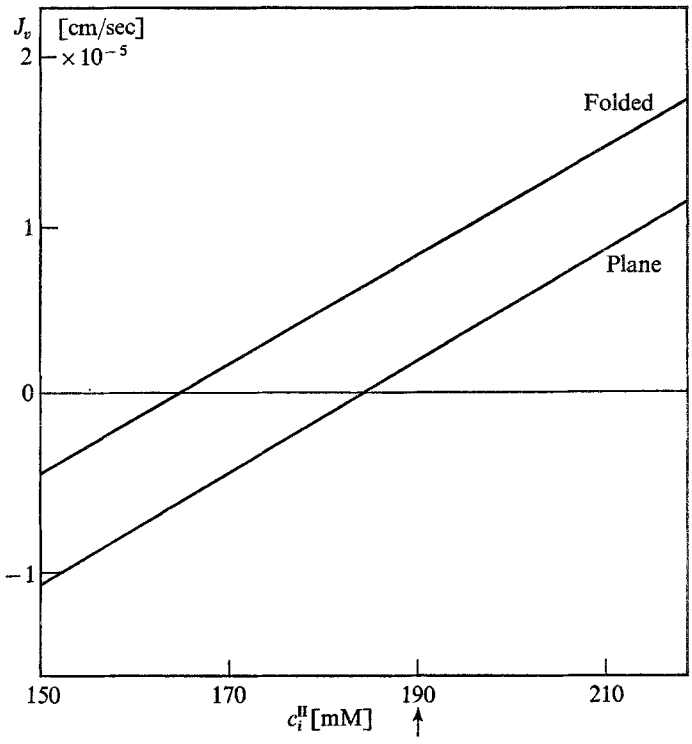


Fig. 8. The volume flow as a function of the concentration of the impermeant species in reservoir II, $C_i^{II}$

impermeant species remains essentially constant in regions $\alpha$ and $\beta$, having the value given in bathing solution I or II. As shown in Fig. 3*a*, the salt concentration in region $\alpha$ decreases from 150 to 135 mM, a drop of 10%. This 10% variation is sufficient to cause a volume flow $3^1/_4$ times greater than would be expected from just the increase in area. It must be recalled that for the plane membrane there is an 8-milliosmole osmotic driving force; in the folded membrane, for $\sigma = 0.7$, the 10% variation in the salt concentration in region $\alpha$ corresponds to an osmotic driving force change of $0.7 \times 15 = 10.5$ milliosmoles. Therefore, the effects of the microstructure should be greatest for nearly isotonic systems, as indeed is the case. The effects of varying $C_i^{II}$ are illustrated in Fig. 8 by plotting the volume flow itself, rather than the flow ratio; this is to avoid the introduction of an apparent singularity in the ratio at $J_V = 0$. The significant feature of this figure is that the isotonic state for the folded membrane does not coincide with that for the plane membrane. To get an idea of the magnitude of this shift, consider the point $C_i^{II} = 182$ mM, where $J_V = 0$ for the plane membrane;

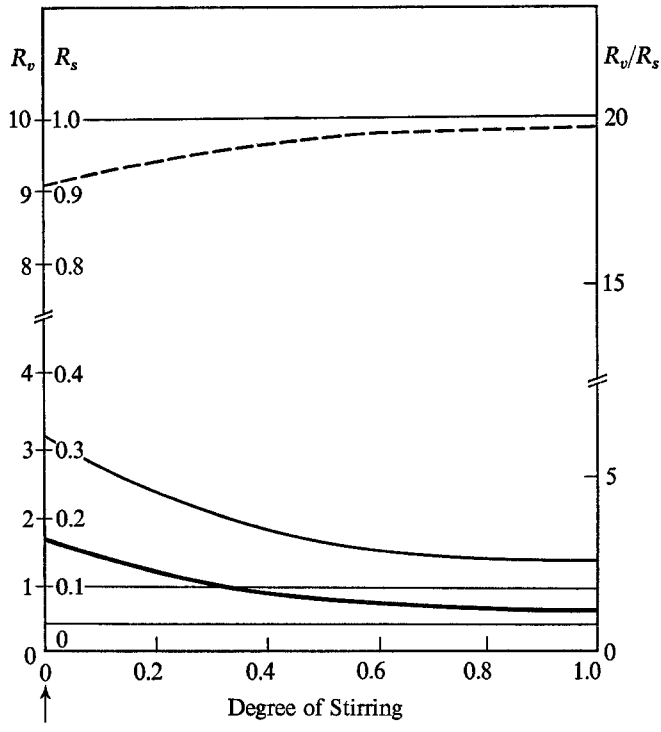


Fig. 9. The flow ratios as functions of the degree of stirring in region $\alpha$. The narrow line is $R_V$; the dashed line is $R_s$; and the wide line is $R_V/R_s$

here $J_V = 7 \times 10^{-6}$ cm/sec for the folded membrane. To achieve this flow of $7 \times 10^{-6}$ cm/sec in the plane membrane $C_i^{II}$ would have to be increased to 200 mM, a substantial increment in biological systems.

### *Effects of Stirring*

Fig. 3 shows the effect upon the salt-concentration profiles caused by stirring region $\alpha$ down to a depth of $0.4\,L$. Fig. 9 shows the effect of stirring upon the flow ratios.

## Discussion

To a great extent a knowledge of the form of the characteristic roots is more valuable than the solution itself, for they provide effective and simple criteria for deciding if the qualitative behavior of a given folded membrane will differ from that of a plane membrane. The system is governed by a single characteristic length $1/\lambda$ given by Eq. (17), which in our "standard"

case has the value $1/\lambda \cong 4$ μ. Thus the "standard" value of $L = 2$ μ is comparable to the characteristic length, and it is to be expected that a concentration profile will be established in regions $\alpha$ and $\beta$.

This study originated in the problem of flows through structured biological membranes such as the microvilli of the intestine and the proximal tubule, and it seemed reasonable initially to limit the analysis to a single permeant salt. It happens that the system equations apply also to a permeant nonelectrolyte because of the condition of zero current flow. The next step in the evolution of the model will be to allow the inter-diffusion of two salts such as NaCl and KCl across the membrane. It is hoped that this may give some insights into the mechanism of isotonic flows. Unlike Diamond and Bossert's (1967) *standing-gradient* flow, which is physically constrained (*see* Segel, 1970) to give a more or less isotonic flow, the isotonicity of the flow in our single-salt folded membrane system is a wide-ranging function of the system parameters. It should be noted that ours is a passive, not an active, transport system. The resemblance of folded membranes to the *standing-gradient* system stems primarily from the fact that time-independent concentration gradients are established in all steady-state diffusion systems.

Most biological systems are maintained in a close neighborhood of isotonicity, and it is in this region that the effects of augmented water flows in tightly folded membranes are found. However, as demonstrated by the example presented in the section *Role of the Impermeant Species*, the isotonic state itself is determined by the membrane geometry, in addition to the membrane permeabilities and solution osmolarities. Folded membrane structures show features of solute and water flow which are qualitatively different from the expected, strictly quantitative effect of increased surface area. The system displays striking nonlinear behavior, sensitive to small changes in the geometry and the permeability coefficients. Thus, the brush border epithelium of many cells could represent a device capable of enhancing or dampening flows by virtue of structural or permeability changes induced by substances such as hormones. And even as static structures, folded membranes may play a role in the concentration of solutions.

## Appendix I

Encountering a nonlinear system of ordinary differential equations with rather unusual boundary conditions, we resorted to digital computer techniques for their solution. A simple rectangular integration procedure sufficed to give rapid convergence. The integration depended upon values of the free boundary conditions $C_s^\beta(0)$ and $C_i^\beta(0)$, which were adjusted by

iteration until the integrated values of $C_s^\beta(L)$ and $C_i^\beta(L)$ agreed with the given values of these boundary conditions. Using Eq. (3) it was necessary to choose the free boundary value $dC_s^\alpha(0)/dx$ so that the integration satisfied two flux conservation statements: (1) the flux of salt into the top of the structure must equal that out the bottom, and (2) the volume flux in must equal that out. Finally, $dC_s^\beta(0)/dx$ was forced to satisfy the flow continuity Eq. (13). Computations were performed on a PDP-12 digital computer using FOCAL 8-1969 language.

## Appendix II

If the salt flow is not coupled by convection to volume flow, Eqs. (6) and (7) reduce to

$$-D_s\frac{d^2C_s^\alpha}{dx^2}+\frac{2RT\omega}{a}(C_s^\alpha-C_s^\beta)=0$$

and (14)

$$-D_s\frac{d^2C_s^\beta}{dx^2}-\frac{2RT\omega}{b}(C_s^\alpha-C_s^\beta)=0,$$

which lead to an ordinary linear homogeneous equation with constant coefficients:

$$\frac{d^4C_s^\alpha}{dx^4}-(p_1+p_2)\frac{d^2C_s^\alpha}{dx^2}=0 \tag{15}$$

with

$$p_1=2RT\omega/aD_s \quad \text{and} \quad p_2=2RT\omega/bD_s.$$

The characteristic equation

$$\lambda^4-(p_1+p_2)\lambda^2=0 \tag{16}$$

has one double and two distinct roots:

$$\lambda_1=0, \qquad \lambda_2=0,$$

$$\lambda_3=+\lambda, \qquad \lambda_4=-\lambda$$

where

$$\lambda=\left[\frac{2RT\omega}{D_s}\left(\frac{1}{a}+\frac{1}{b}\right)\right]^{\frac{1}{2}}. \tag{17}$$

Thus the solution of Eq. (14) is

$$C_s^\alpha=A_1+A_2x+A_3e^{\lambda x}+A_4e^{-\lambda x}$$

and (18)

$$C_s^\beta=A_1+A_2x+\left(1-\frac{\lambda^2}{p_1}\right)(A_3e^{\lambda x}+A_4e^{-\lambda x})$$

where the four integration constants are determined from the following boundary conditions:

$$\begin{aligned} C_s^{\alpha}(0) &= C_s^{\mathrm{I}} \\ C_s^{\beta}(L) &= C_s^{\mathrm{II}} \\ \frac{dC_s^{\alpha}(L)}{dx} &= -\frac{2RT\omega}{D_s}[C_s^{\alpha}(L) - C_s^{\beta}(L)] \\ \frac{dC_s^{\beta}(0)}{dx} &= -\frac{2RT\omega}{D_s}[C_s^{\alpha}(0) - C_s^{\beta}(0)]. \end{aligned} \tag{19}$$

I.W.R.'s contribution to this work was done during the tenure of a Visiting Scientist Award of the American Heart Association. V.L. was supported by NIH Grant No. GM17539. E.B. was supported by NIH Grant No. AM16187 and by NASA Grant No. NGR05-025-007.

## References

Diamond, J. M., Bossert, W. H. 1967. Standing-gradient osmotic flow. *J. Gen. Physiol.* **50**:2061.

Kedem, O., Katchalsky, A. 1963. Permeability of composite membranes: Part I. *Trans. Faraday Soc.* **59**:1918.

Segel, L. A. 1970. Standing-gradient flows driven by active solute transport. *J. Theoret. Biol.* **29**:233.